

B2

Special Report - 1

Edge-cracks in T-butt weld:

*Convergence and verification,
modelling strategies for microscopic to
macroscopic cracks.*

Michael Forster

4 July 1995

B2 1.01

© Copyright Michael Forster, 1995. All rights reserved.

No part of this report may be reproduced or transmitted in any form or by any means, for any purpose without the express written permission of Michael Forster.

Contents

1. General remarks (p. 4 - 8)
2. Convergence and verification study on a microscopic straight edge-crack in a rectangular plate (p. 9 - 12)
3. Convergence study on a microscopic straight crack in a T-butt weld joint (p. 13 - 16)
4. Comparison of B2 and FEA results for straight cracks of different lengths in the corner of a T-butt weld joint (p. 17 - 21)
5. Determination of the most likely location and angle of crack initiation at the edge of a profiled T-butt weld joint (p. 22)
6. Comparison of results for straight and curved cracks of different lengths, which initiate at the most likely location of a profiled T-butt weld joint (p. 23 - 28)

Disk directories:	Session files:	Description:
\edgecrak	s20006xx.bem	edge-crack in rectangular plate
\tbutt\straight\conv	s20002xx.bem	t-joint, convergence study
\tbutt\straight\corner	s20003xx.bem	t-joint, FEA comparison
\tbutt\straight	s20005xx.bem	t-joint, most likely straight crack
\tbutt\curve	s20004xx.bem	t-joint, most likely curved crack

1. General remarks

Overview

This report demonstrates how to obtain highly accurate stress intensity factors in edge-crack analyses, for crack lengths ranging from microscopic to macroscopic.

A microscopic straight edge crack in a rectangular plate is analysed with different crack meshes to determine the convergence of results and to compare them with published results.

A T-butt weld joint with a microscopic straight edge crack is analysed with different meshes and shows that convergence is the same as for the above example. Based on one of the "converged" meshes, stress intensity factors are computed for a range of crack lengths and compared with published solutions obtained by finite element analysis for the British Standard BS PD 6493.

Finally, an analysis of an uncracked t-joint is carried out to determine the most likely location of crack initiation and the most likely initial crack direction. Then, cracks of different lengths are introduced accordingly.

Running the analyses yourself

Included in this report are disks with data files corresponding to the analyses tabled in the following chapters of this report. They must be copied onto harddisk before they can be used.

- B2 session files SXXXXXXXX.BEM, where XXXXXXXX is the session ID.
- AXXX.DAT data files for the solver. The first 4 digits of the session ID were truncated, eg A204.DAT corresponds to session 2000204.
- Batch files (BAT) to run a batch of analyses. The BAT-files start the B2-solver PLANE on a batch of AXXX.DAT data files.

The solver produces results files with the extensions LUP, LUZ, and OUT. The LUP and LUZ files are for importing results into B2 and can be discarded. The OUT files contain tabled results and can be printed out or viewed with a text editor.

A text editor is the fastest method to examine the OUT files. Its search function can be used to search for specific element numbers, or for "SING" to find the stress singularities.

Load cases

Load case commands are not yet available in the B2 1.01 menus, but the session files contain the results for two load cases and the B2-solver PLANE handles up to 5 load-cases. So results graphics for both load cases can be viewed with later versions of B2.

An additional load case was defined by editing Axxx.DAT with a text editor. The first load case was renamed to Tension and the new load case was called Bending.

The load values are preceded by the keyword TE and are arranged in the same way as entered at the **Force per unit length** command (**BC** menu), taking into account the orientation of the elements. The next line contains the keyword EL and the element-number for which the load was defined.

```
T_000002000204 2000204 G 1D 1M 1BC 1 2096
...
...
L Tension
TE 1.00000000 .000000000
EL 19
TE -1.00000000 .000000000
EL 18
L Bending
TE -1.00000000 .000000000 1. 0.
EL 19
TE -1.00000000 .000000000 1. 0.
EL 18
END
```

A204.DAT

How to create DAT files and read results into B2

- Create the data file for the solver using the command **Write PLANE.DAT; no run (PLANE menu)**.
- Exit B2 and rename PLANE.DAT to e.g. A204.DAT
- Use a text editor to add a load-case.
- Run the solver from the DOS prompt by typing PLANE A204 or run the batch of analyses by typing TCONV R
- Before importing the results into the B2 parent session, rename the LUP and LUZ file to PLANE.LUP and PLANE.LUZ and copy them to the directory \B2.
- Start B2 and load the parent session.
- Use **Read PLANE.OUT (PLANE menu)** to read the results from PLANE.LUP and PLANE.LUZ. The results for all load cases will be read and stored but B2 1.01 can only display the results of the first load case.

Microscopic details in B2

For certain mouse operations in the crack-tip region, it is necessary to redefine the rounding value to 1.0E-5 mm or so (default is 0.1 mm) using the command **Mouse rounding** (**File** menu).

If you forget to do this, commands such as **Mousepoint** or **Scale-bar lengths** will not work as expected, as the coordinates defined by the mouse are rounded to a multiple of the rounding-value.

If a solver-run is unsuccessful and you find the message "Zero Jacobian, element ..." in the file PLANE.OUT, this element was too small with respect to the overall dimensions of the subregion or single-subregion model. In B2 1.01 the thresholds for this condition were lowered and this message is unlikely.

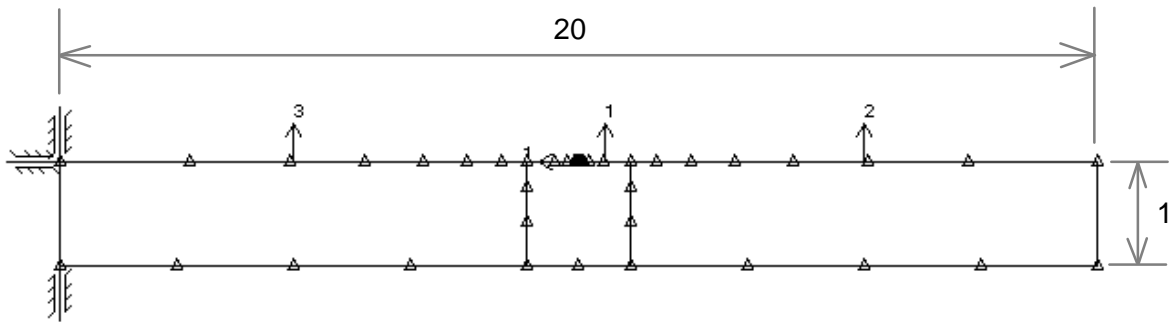
Work-around: Encapsulate any such detail within a smaller subregion. The thresholds are dynamic, so an element may be smaller if the subregion it belongs to is smaller.

For the analyses in this report, subregions were used to cut solution time and reduce round-off error. Surprisingly however, no round-off problems were encountered when single-subregion analyses were run.

With crack sizes 20,000 times smaller than the base plate length, and crack-tip elements 200,000 times smaller than the longest elements or 4,000,000 times smaller than the base plate length, the results of single-subregion analyses were within 0.2% of those using multiple subregions.

In other words, the following analyses can be run with single-subregion meshes without numerical problems.

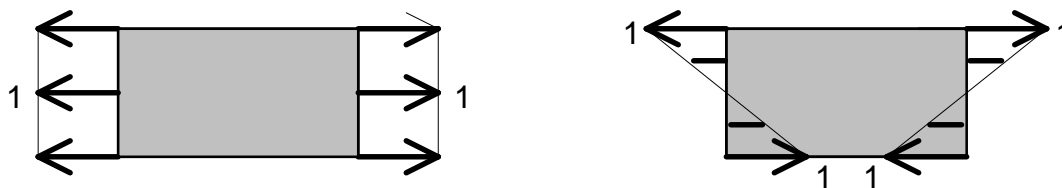
2. Convergence and verification study on a microscopic straight edge-crack in a rectangular plate



The figure shows a rectangular 20 x 1 plate. It is divided into 3 subregions, as shown by the outward normal vector of each subregion. The crack is at the top surface of subregion 1 and the crack outward normal can only just be seen, parallel to the upper boundary.

At the left hand side of the plate there are 3 point constraints which prevent rigid body translation and rotation. They cannot take any reaction forces, but allow different load cases with self-equilibrating loads to be defined.

Two load cases are considered, unit membrane tension and unit beam bending stress:



Elastic constants:

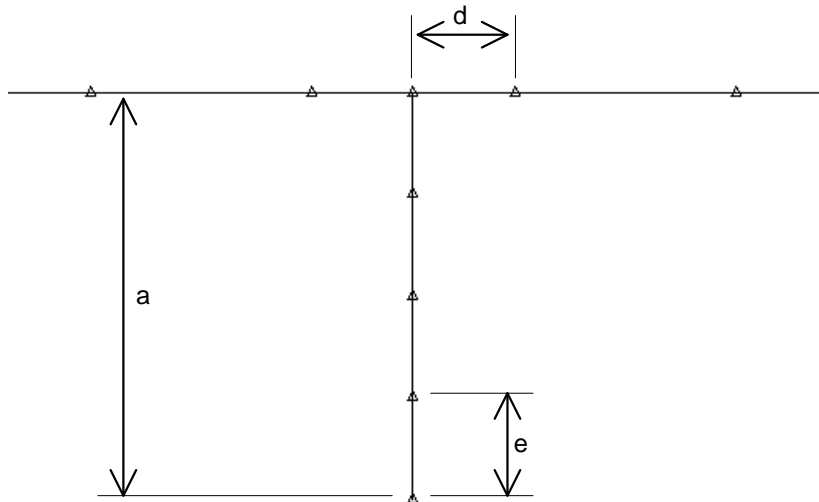
$$E = 210\,000 \text{ N/mm}^2$$

$$\nu = 0.3$$

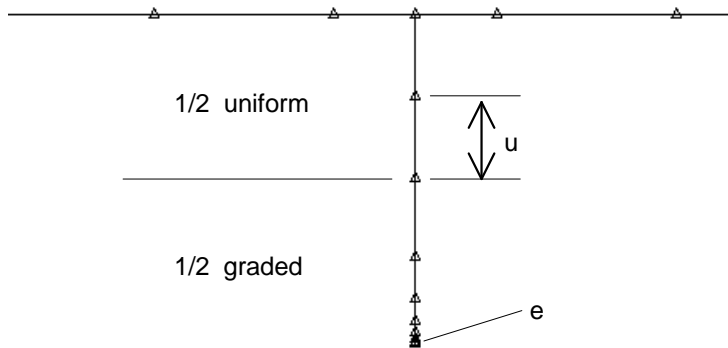
Plane strain

Crack detail

Crack with uniform elements:



Crack with graded elements:



a: crack length. $a = 0.001$

d: element length next to crack root

e: element length at crack tip

u: element length on uniform part of crack with graded crack-tip mesh

Crack length $a = 0.001$:

The stress intensity factor K_I is normalised as follows:

$Y_I = K_I / \sigma\sqrt{\pi a}$, where σ is the boundary tangential stress very far from the crack

Crack with uniform elements:

Session	elements per crack face	e in a	d in a	K_I Tension 0.01 N/mm ^{1.5}	K_I Bending 0.01 N/mm ^{1.5}	Y_I Tension	Y_I Bending
2000601	1	1.0	0.5	6.0512	6.0435	1.0796	1.0782
2000602	1	1.0	0.25	6.2224	6.2143	1.1102	1.1087
2000603	2	0.5	0.25	6.2936	6.2858	1.1229	1.1215
2000604	4	0.25	0.25	6.2912	6.2836	1.1224	1.1211
2000605	8	0.125	0.5	6.2825	6.2749	1.1209	1.1195
2000606	8	0.125	0.25	6.2888	6.2812	1.1220	1.1206
2000607	8	0.125	0.15	6.2884	6.2808	1.1219	1.1206
2000608	8	0.125	0.075	6.2885	6.2809	1.1219	1.1206

Crack with graded elements:

On the graded crack half, 7 elements per crack face with crack tip element graded to length $e = 0.005a$

Session	uniform elements per face	u in a	d in a	K_I Tension 0.01 N/mm ^{1.5}	K_I Bending 0.01 N/mm ^{1.5}	Y_I Tension	Y_I Bending
2000609	1	0.5	0.5	6.2452	6.2430	1.1142	1.1138
2000610	2	0.25	0.25	6.2882	6.2852	1.1219	1.1214
2000611 1 subregion	2	0.25	0.25	6.2872		1.1217	

Murakami:

T. Murakami, "Stress Intensity Factors Handbook", Pergamon Press, Oxford 1987, gives two approximate solutions for very short edge-cracks as a function of the boundary tangential stress very far from the crack:

$$1) K_I = 1.12 \sigma\sqrt{\pi a} = 6.278 \text{ N / mm}^{1.5} \text{ for } a = 0.001$$

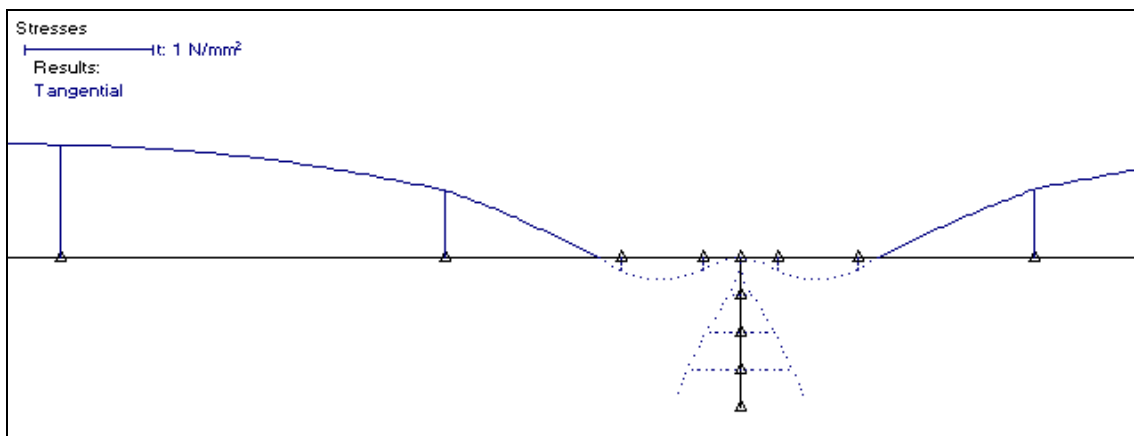
$$2) K_I = 1.122 \sigma\sqrt{\pi a} = 6.289 \text{ N / mm}^{1.5} \text{ for } a = 0.001$$

This is in very close agreement with the above results, ie within 0.01% for the 2nd reference value and the fine B2 meshes under tension.

Guidelines for mesh design of straight edge-cracks can be summarised as follows:

1. The stress intensity factors converge for 8 elements per crack-face and an adjacent element length of $d = 0.25a$.
2. For 8 elements per crack face and $d = 0.5a$, the solution deteriorates by 0.1%, for less crack elements, it deteriorates more drastically.
3. For 4 elements per crack face and $d = 0.25a$, the solution only deteriorates by 0.04%.
4. The element size on the crack at the crack root needs to be $u = 0.25a$. If $u = 0.5a$ the solution deteriorates by 0.7%, and if $u < 0.25a$ there is no further change in the solution.

Note that holes or other causes of stress concentrations very near the crack may require different crack meshes.



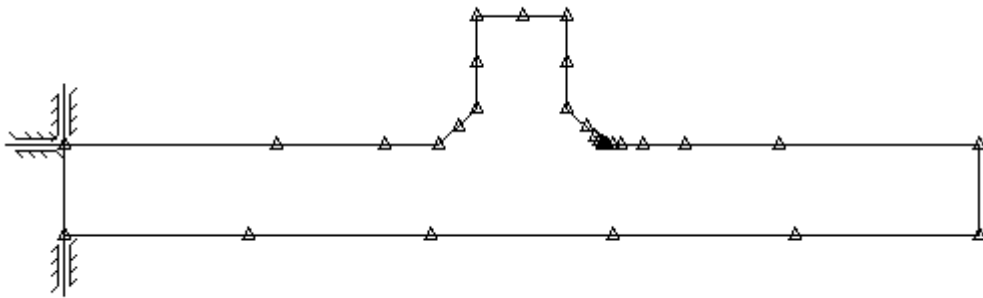
Typical stress distribution at edge cracks

Approaching the crack root, the extreme-fibre stress on the plate boundary changes rapidly from tensile to compressive and back to zero, ie an S-shaped wobble. The tangential stress on the crack-face is compressive. At the crack tip there is a stress singularity, and in the material near the tip there is a very high stress gradient.

3. Convergence study on a microscopic straight crack in a T-butt weld joint

Starting off with a coarse single-subregion boundary element mesh, the mesh was refined and multiple subregions were used.

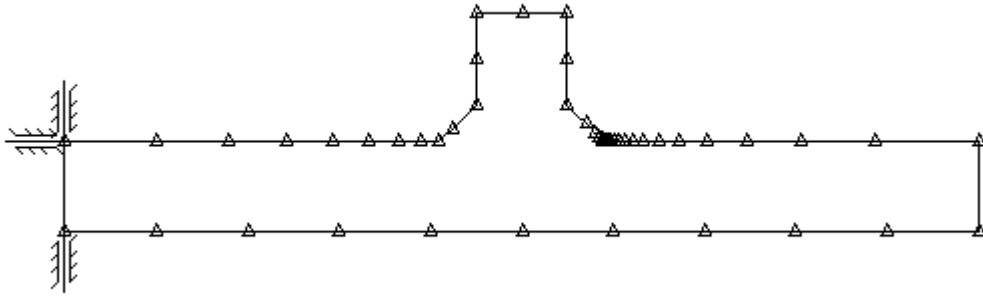
crack length: $a = 0.001$ mm
plate length L: 10 mm (20 mm)
plate thickness T: 1 mm
attachment width t: 1 mm
weld width w: 0.4 mm
weld angle: 45°
attachment height: 1.4 mm



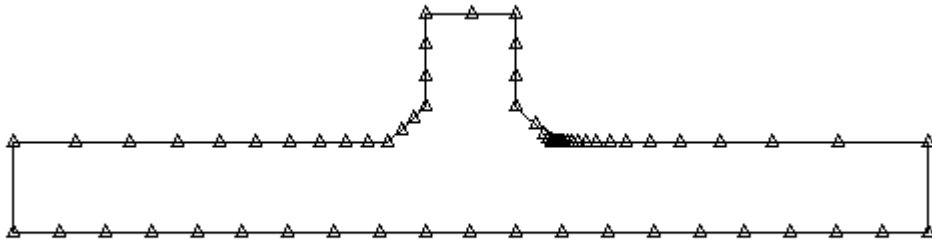
Mesh 1: Coarse global mesh

Elastic constants:
 $E = 210\,000$ N/mm²
 $\nu = 0.3$
Plane strain

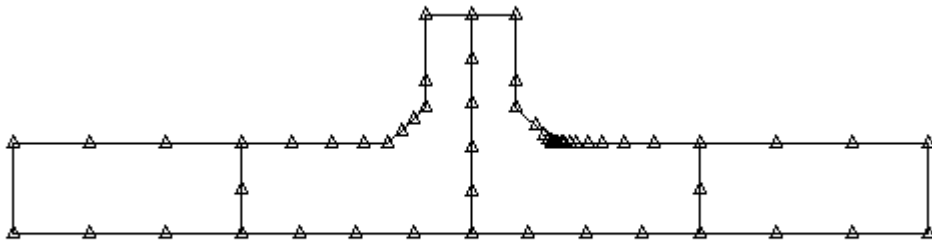
Load cases:
1. membrane tension
2. beam bending



Mesh 2: Medium global mesh



Mesh 3: Fine global mesh

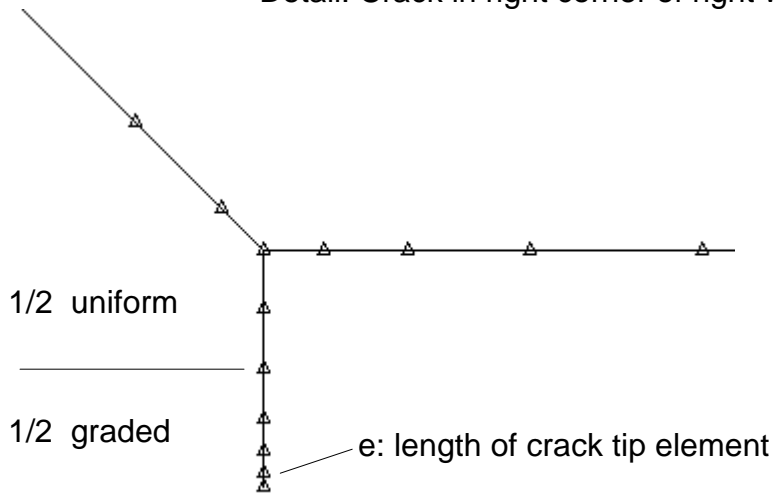


Mesh 4: Multiple subregions. a) 18 interface elements, b) 9 interface elements



Mesh 5: Longer plate (L=20mm)

Detail: Crack in right corner of right weld



Mesh gradation was used to obtain a good transition from the very short crack to the large global details. The crack elements were graded with a term ratio of about 2:1, and the adjoining elements were similarly graded from the length of the longest crack element to the length of a typical element of the global mesh.

The largest element was 200 000 times as large as the smallest crack-tip element, so mesh gradation is necessary for efficiency, and subregioning is advisable.

Results:

Session	mesh	graded elements per crack face	uniform elements per crack face	e in a	K_I in $N/mm^{1.5}$	K_{II} in $N/mm^{1.5}$	Y_I	Y_{II}
2000204	1	0	4	0.25	0.25207	0.050924	4.4972	0.9085
2000207	2	4	2	0.0625	0.23765	0.047842	4.2400	0.8536
2000216	2	6	2	0.02	0.23764	0.047843	4.2398	0.8536
2000209	3	6	2	0.02	0.23697	0.047696	4.2278	0.8510
2000212	4a	6	2	0.02	0.23701	0.047702	4.2286	0.8511
2000214	4a	10	2	0.005	0.23701	0.047709	4.2286	0.8512
2000224	4b	6	2	0.02	0.23705	0.047712	4.2293	0.8512
2000222	5	6	2	0.02	0.23700	0.047700	4.2284	0.8510

T-joint with vertical crack in corner of weld ($a / T = 0.001$), load-case tension

Session	mesh	graded elements per crack face	uniform elements per crack face	e in a	K_I in $N/mm^{1.5}$	K_{II} in $N/mm^{1.5}$	Y_I	Y_{II}
2000204	1	0	4	0.25	0.29307	0.061041	5.2287	1.0890
2000207	2	4	2	0.0625	0.26898	0.055867	4.7989	0.9967
2000216	2	6	2	0.02	0.26906	0.055868	4.8004	0.9968
2000209	3	6	2	0.02	0.26852	0.055742	4.7907	0.9945
2000212	4a	6	2	0.02	0.26848	0.055741	4.7900	0.9945
2000214	4a	10	2	0.005	0.26850	0.055735	4.7904	0.9944
2000224	4b	6	2	0.02	0.26850	0.055749	4.7904	0.9946
2000222	5	6	2	0.02	0.26846	0.055738	4.7897	0.9944

T-joint with vertical crack in corner of weld ($a / T = 0.001$), load-case bending

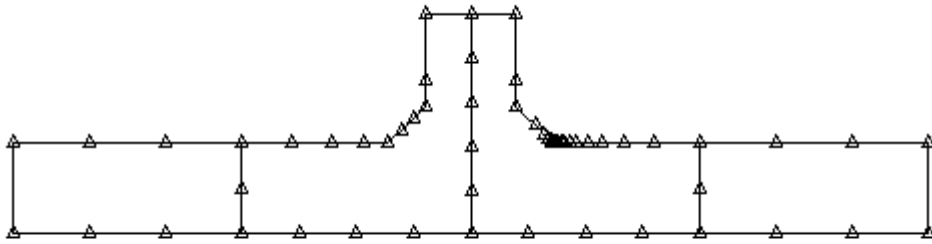
The difference between 4 and 6 elements per crack surface is about 6.0% for tension and 9% for bending. The difference between 6 and 8 crack elements is 0.03% or less for the single-subregion meshes. The difference between a medium global mesh and a fine global mesh is under 0.28%.

The difference between the fine single-subregion mesh and the multiple subregion mesh for 8 crack elements is less than 0.02%.

There is no difference between 8 and 12 elements per crack face and no difference between plate length 20 (mesh 5) and plate length 10 (meshes 1-4).

The difference between the multiple subregion mesh 4a with the fine interface and 4b with the coarse interface is less than 0.017%. Therefore the mesh 4b with 8 crack elements was chosen as the basic mesh design for the analyses with other crack lengths.

4. Comparison of B2 and FEA results for straight cracks of different lengths in the corner of a T-butt weld joint



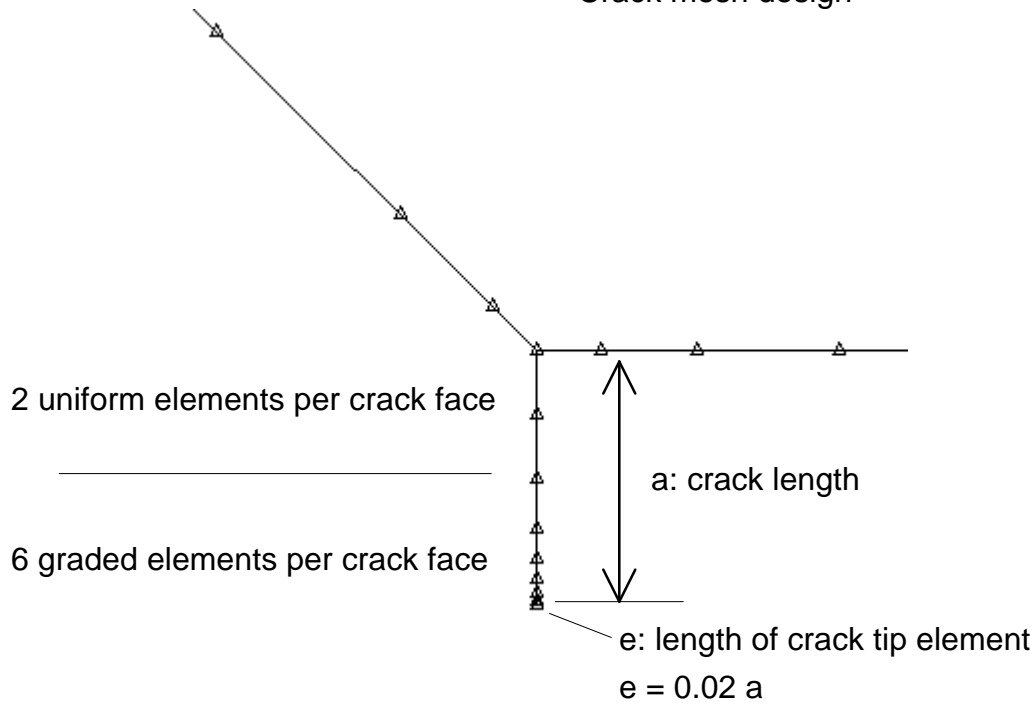
Global mesh design (mesh 4b of convergence study)

plate length L : 10 mm (FEA: 20 mm, but this makes no difference)
plate thickness T : 1 mm
attachment width t : 1 mm
weld width w : 0.4 mm
weld angle: 45°
attachment height: 1.4 mm

Elastic constants:
 $E = 210\,000\text{ N/mm}^2$
 $\nu = 0.3$
Plane strain

Load cases:
1. membrane tension
2. beam bending

Crack mesh design



Results:

Session	a in mm	e in mm	K_I in $N/mm^{1.5}$	K_{II} in $N/mm^{1.5}$	Y_I	Y_{II}	Y_I FEA
2000220	0.001	2.0E-5	0.23701	0.047702	4.2286	0.8511	4.567
2000301	0.002	4.0E-5	0.26894	0.052465	3.3929	0.6619	3.630
2000302	0.004	8.0E-5	0.30639	0.056901	2.7332	0.5076	2.901
2000303	0.006	1.2E-4	0.33163	0.059094	2.4155	0.4304	2.552
2000304	0.008	1.6E-4	0.35146	0.060345	2.2170	0.3806	2.329
2000306	0.010	2.0E-4	0.36814	0.061084	2.0770	0.3446	2.182
2000307	0.020	4.0E-4	0.43008	0.061505	1.7158	0.2454	1.783
2000308	0.030	6.0E-4	0.47676	0.059940	1.5530	0.1952	1.602
2000309	0.040	8.0E-4	0.51727	0.057731	1.4592	0.1629	1.500
2000310	0.060	1.2E-3	0.59023	0.052854	1.3595	0.1217	1.385
2000311	0.080	1.6E-3	0.65914	0.047983	1.3148	0.0957	1.337
2000312	0.100	2.0E-3	0.72750	0.043360	1.2980	0.0774	1.317
2000313	0.120	2.4E-3	0.79723	0.039179	1.2984	0.0638	1.313
2000314	0.140	2.8E-3	0.86938	0.035358	1.3109	0.0533	1.326
2000315	0.160	3.2E-3	0.94480	0.031871	1.3326	0.0450	1.347
2000316	0.180	3.6E-3	1.02420	0.028721	1.3620	0.0382	1.377
2000317	0.200	4.0E-3	1.10810	0.025871	1.3979	0.0326	1.402
2000318 mesh 4a with 18 interface elements	0.200	4.0E-3	1.10810	0.025883	1.3979	0.0327	1.402

T-joint with vertical crack in corner of weld, mesh 4b, load-case tension

Session	a in mm	e in mm	K_I in N/mm ^{1.5}	K_{II} in N/mm ^{1.5}	Y_I	Y_{II}	Y_I FEA
2000226	0.001	2.0E-5	0.26847	0.055740	4.7898	0.9945	5.156
2000301	0.002	4.0E-5	0.30356	0.062154	3.8296	0.7841	4.116
2000302	0.004	8.0E-5	0.34383	0.068838	3.0672	0.6141	3.283
2000303	0.006	1.2E-4	0.37024	0.072729	2.6967	0.5297	2.870
2000304	0.008	1.6E-4	0.39049	0.075398	2.4631	0.4756	2.611
2000306	0.010	2.0E-4	0.40716	0.077376	2.2972	0.4365	2.439
2000307	0.020	4.0E-4	0.46569	0.082511	1.8578	0.3292	1.957
2000308	0.030	6.0E-4	0.50611	0.084329	1.6486	0.2747	1.725
2000309	0.040	8.0E-4	0.53874	0.084752	1.5198	0.2391	1.585
2000310	0.060	1.2E-3	0.59246	0.083741	1.3646	0.1929	1.409
2000311	0.080	1.6E-3	0.63847	0.081496	1.2736	0.1626	1.314
2000312	0.100	2.0E-3	0.68068	0.078649	1.2144	0.1403	1.246
2000313	0.120	2.4E-3	0.72108	0.075605	1.1744	0.1231	1.199
2000314	0.140	2.8E-3	0.76071	0.072422	1.1470	0.1092	1.170
2000315	0.160	3.2E-3	0.80030	0.069164	1.1288	0.0976	1.150
2000316	0.180	3.6E-3	0.84037	0.065915	1.1175	0.0877	1.137
2000317	0.200	4.0E-3	0.88132	0.062684	1.1118	0.0791	1.118
2000318 mesh 4a with 18 interface elements	0.200	4.0E-3	0.88134	0.062698	1.1119	0.0791	1.118

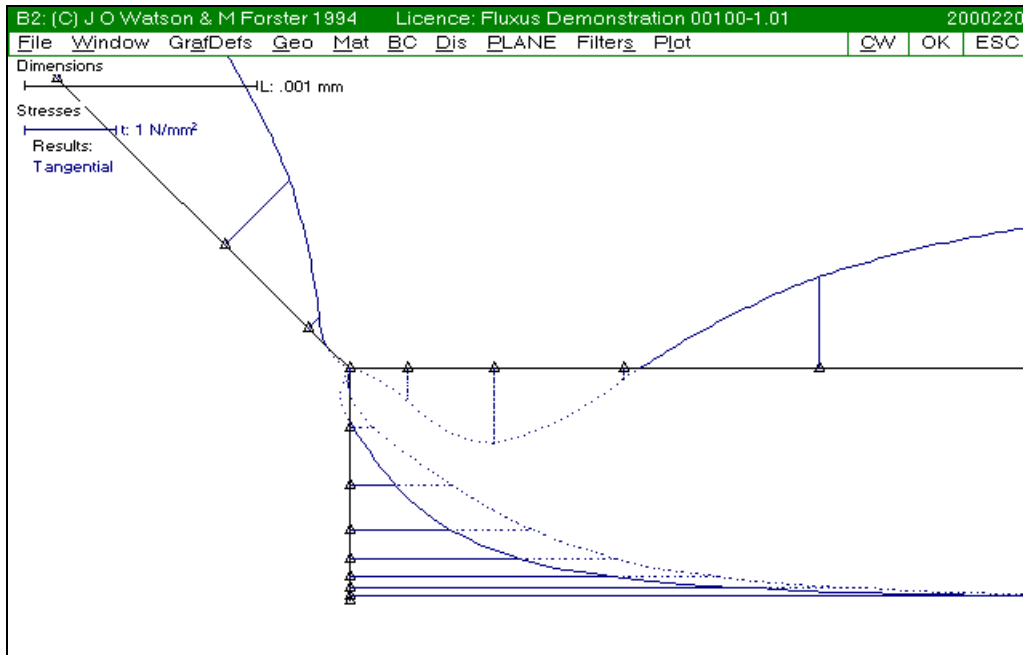
T-joint with vertical crack in corner of weld, mesh 4b, load-case bending

The mode-II stress intensity factor is quite significant for normalised crack-lengths less than 0.100 in tension and for all crack lengths in bending. According to the principal stress criterion, cracks orient their path of growth such that the mode-II component becomes insignificant.

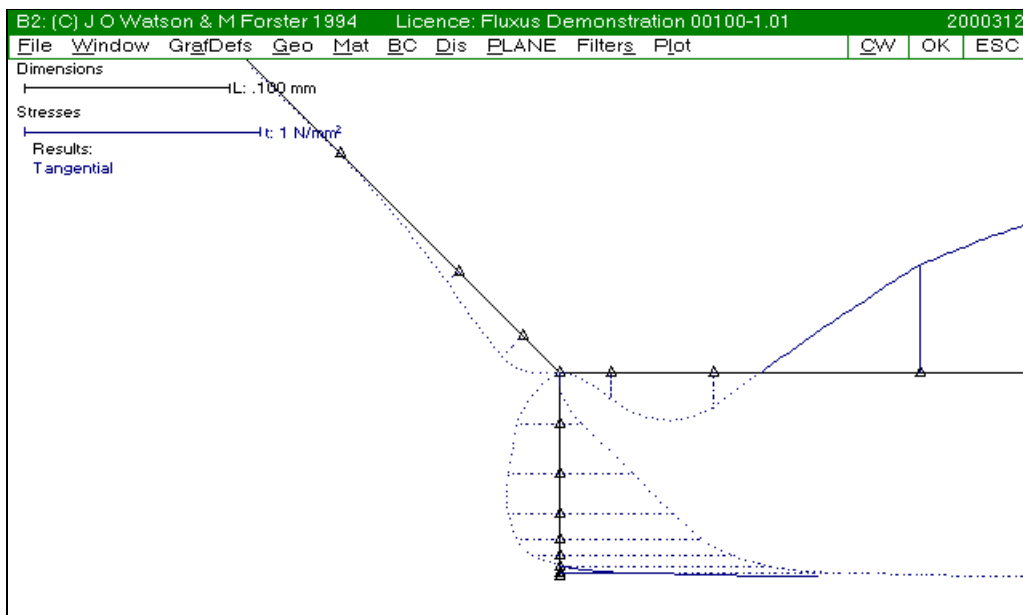
Comparing boundary element results and FEA-results, the FEA-results are about 6%-9% higher for very short crack lengths and about 1%-2% higher for long cracks. Probably the FE-mesh for short cracks was too coarse, as a coarse boundary element mesh showed a similar tendency (T-butt convergence runs for a = 0.001, session 2000204).

The finite element analyses were carried out by I.J. Smith and S.J. Hurworth at The Welding Institute (England) and the results were incorporated into the old British Standard BS PD 6493 : 1991. The standard is currently being updated.

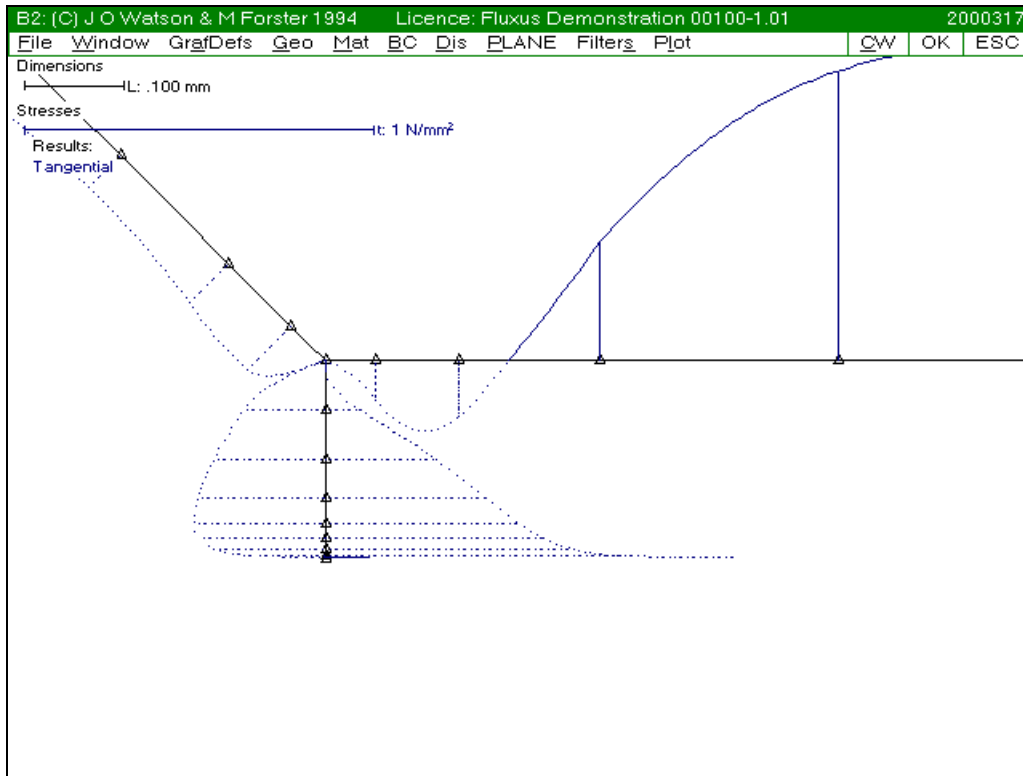
The FEA results are not to such a high accuracy as the B2 results, because the meshes of cubic finite elements were much coarser than the B2 meshes. Also, the FEA results for the rectangular plate with edge cracks of different lengths showed an error of between 1% and 2% compared to Murakami.



Crack length 0.001mm. Note strongly asymmetric crack stress distribution, which indicates a strong mode-II crack opening component.

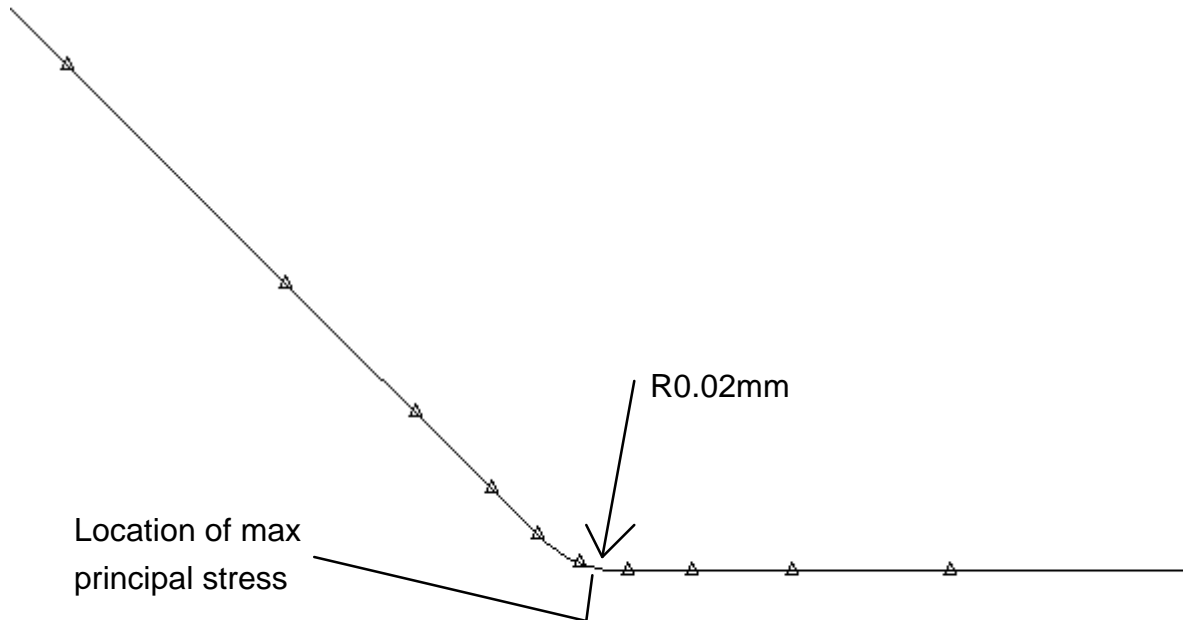


Crack length 0.100mm. Crack stress distribution more symmetric.



Crack length 0.200mm. Crack stresses nearly symmetric.

5. Determination of the most likely location and angle of crack initiation at the edge of a profiled T-butt weld joint



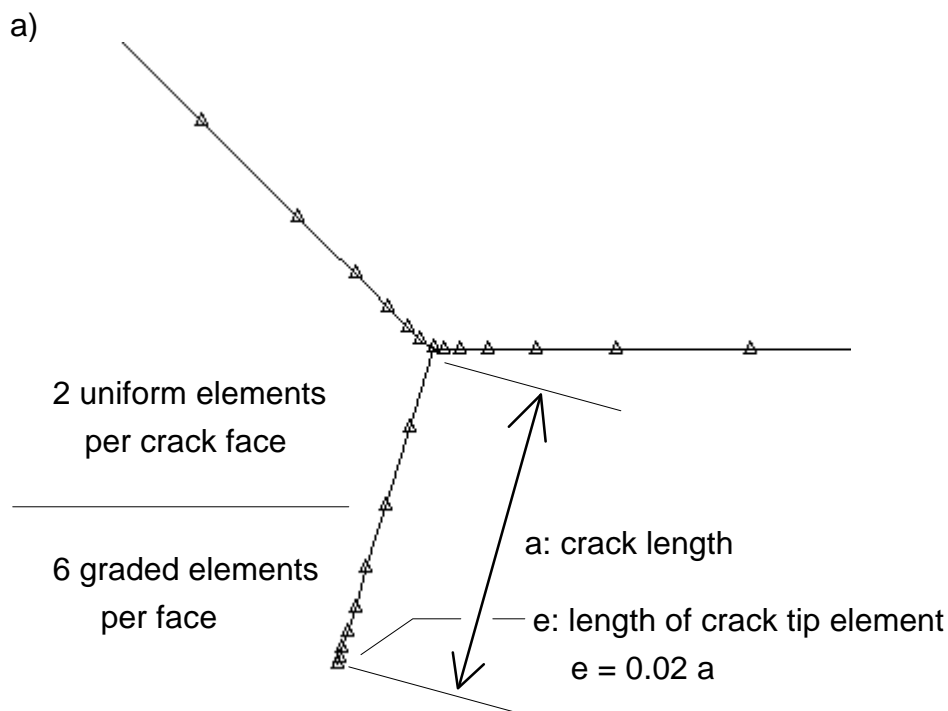
Session 2000401: A radius of 0.02 mm was applied to the edge of the weld. A boundary element analysis of the uncracked t-joint was performed.

Elastic properties of mild steel under plane strain were used as for the previous analyses. Load cases membrane tension and beam bending were applied as before.

The location of highest principal stress in the radius was identified at about 3/8 of the arc measured from the vertical, ie at 16.875°. This is the angle at which a crack would start according to the maximum principal stress criterion, because the direction of max principal stress is identical to the boundary tangent in the absence of applied stresses to the boundary. The angle is practically the same for tension and bending.

6. Comparison of results for straight and curved cracks of different lengths, which initiate at the most likely location of a profiled T-butt weld joint

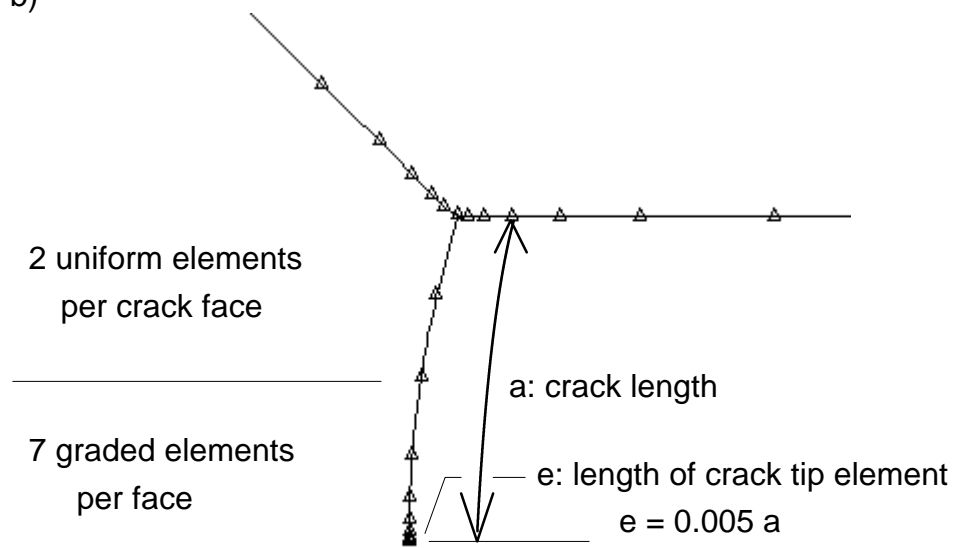
Two cases of crack geometry were analysed:



Straight crack starting in the radius at the edge of the weld, perpendicular to the angle of max principal stress in the radius. The radius is 0.02mm as for the preceding uncracked t-joint.

N.B.: The mesh cannot be coarser in the region of the crack root, because already only 1 arc element was used on each side of the crack root to model the weld radius. The adjacent elements are graded taking into account the rule that the term ratio should not exceed 2:1. Accuracy is not impaired by the crack root mesh.

b)



Curved crack starting in the radius at the edge of the weld, perpendicular to the angle of max principal stress. The curvature radius of the crack was chosen to be 0.68mm, so that for a crack depth of 0.2mm the crack-tip tangent is vertical, as the straight vertical crack showed practically pure mode-I crack opening for a length of 0.2mm.

There are 2 uniform elements plus 7 graded elements with a term ratio of about 2:1, because an arc-shaped crack in infinite elastic space required 8 graded elements from middle to crack-tip for analytical accuracy.

Elastic properties of mild steel under plane strain were used as for the previous analyses. Load cases membrane tension and beam bending were applied as before.

a) results for tension

a in mm	Session straight crack	e in mm	K_I in $N/mm^{1.5}$	K_{II} in $N/mm^{1.5}$	Session curved crack	e in mm	K_I in $N/mm^{1.5}$	K_{II} in $N/mm^{1.5}$
0.001	2000501	2.0E-5	0.18318	5.287E-4	2000405	5.0E-6	0.18379	6.850E-4
0.004	2000504	8.0E-5	0.29621	2.330E-3	2000407	2.0E-5	0.29614	3.307E-3
0.008	2000506	1.6E-4	0.35298	1.431E-3	2000409	4.0E-5	0.35293	3.735E-3
0.010	2000508	2.0E-4	0.37142	7.154E-5	2000411	5.0E-5	0.37142	3.106E-3
0.020	2000510	4.0E-4	0.43366	-9.251E-3	2000413	1.0E-4	0.43415	-2.098E-3
0.040	2000513	8.0E-4	0.51418	-2.843E-2	2000415	2.0E-4	0.51701	-1.115E-2
0.080	2000515	1.6E-3	0.64013	-6.481E-2	2000417	4.0E-4	0.65171	-2.039E-2
0.120	2000517	2.4E-3	0.76175	-9.887E-2	2000419	6.0E-4	0.78612	-1.767E-2
0.160	2000519	3.2E-3	0.89174	-1.320E-1	2000421	8.0E-4	0.93152	-3.179E-3
0.200	2000521	4.0E-3	1.03570	-1.652E-1	2000423	1.0E-3	1.09210	2.358E-2

T-joint with angled crack in corner of weld, mesh 4b, load-case tension

Normalised stress intensity factors for load case tension:

a in mm	Session straight crack	e in mm	Y_I straight	Y_{II} straight	Session curved crack	e in mm	Y_I curved	Y_{II} curved
0.001	2000501	2.0E-5	3.2681	0.0094	2000405	5.0E-6	3.2790	0.0122
0.004	2000504	8.0E-5	2.6424	0.0208	2000407	2.0E-5	2.6418	0.0295
0.008	2000506	1.6E-4	2.2265	0.0090	2000409	4.0E-5	2.2262	0.0236
0.010	2000508	2.0E-4	2.0955	0.0004	2000411	5.0E-5	2.0955	0.0175
0.020	2000510	4.0E-4	1.7301	-0.0369	2000413	1.0E-4	1.7320	-0.0084
0.040	2000513	8.0E-4	1.4505	-0.0802	2000415	2.0E-4	1.4585	-0.0315
0.080	2000515	1.6E-3	1.2769	-0.1293	2000417	4.0E-4	1.3000	-0.0407
0.120	2000517	2.4E-3	1.2406	-0.1610	2000419	6.0E-4	1.2803	-0.0288
0.160	2000519	3.2E-3	1.2578	-0.1862	2000421	8.0E-4	1.3139	-0.0045
0.200	2000521	4.0E-3	1.3066	-0.2084	2000423	1.0E-3	1.3778	0.0297

T-joint with angled crack in corner of weld, mesh 4b, load-case tension

b) results for bending

a in mm	Session straight crack	e in mm	K_I in $N/mm^{1.5}$	K_{II} in $N/mm^{1.5}$	Session curved crack	e in mm	K_I in $N/mm^{1.5}$	K_{II} in $N/mm^{1.5}$
0.001	2000501	2.0E-5	0.20676	1.232E-3	2000405	5.0E-6	0.20737	1.426E-3
0.004	2000504	8.0E-5	0.33394	6.356E-3	2000407	2.0E-5	0.33381	7.450E-3
0.008	2000506	1.6E-4	0.39657	9.410E-3	2000409	4.0E-5	0.39633	1.198E-2
0.010	2000508	2.0E-4	0.41638	9.758E-3	2000411	5.0E-5	0.41610	1.312E-2
0.020	2000510	4.0E-4	0.47999	7.585E-3	2000413	1.0E-4	0.47952	1.531E-2
0.040	2000513	8.0E-4	0.55274	-1.501E-4	2000415	2.0E-4	0.55243	1.752E-2
0.080	2000515	1.6E-3	0.64583	-1.747E-2	2000417	4.0E-4	0.64715	2.336E-2
0.120	2000517	2.4E-3	0.72015	-3.427E-2	2000419	6.0E-4	0.72441	3.321E-2
0.160	2000519	3.2E-3	0.79031	-5.474E-2	2000421	8.0E-4	0.79822	4.700E-2
0.200	2000521	4.0E-3	0.86158	-6.625E-2	2000423	1.0E-3	0.87328	6.472E-2

T-joint with angled crack in corner of weld, mesh 4b, load-case bending

Normalised stress intensity factors for load case bending:

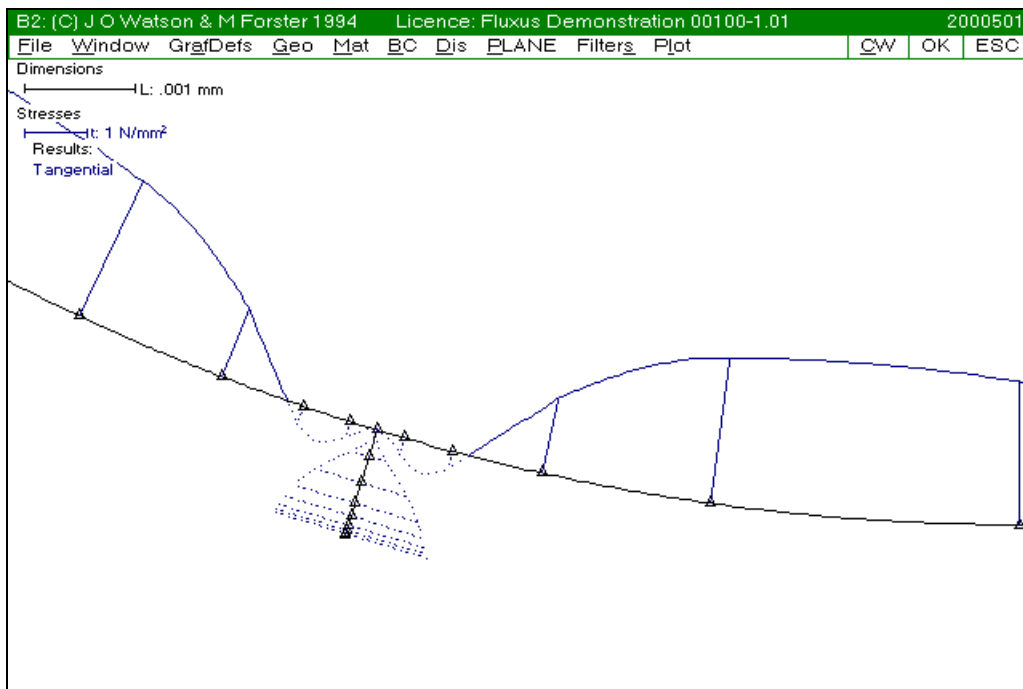
a in mm	Session straight crack	e in mm	Y_I straight	Y_{II} straight	Session curved crack	e in mm	Y_I curved	Y_{II} curved
0.001	2000501	2.0E-5	3.6889	0.0220	2000405	5.0E-6	3.6997	0.0254
0.004	2000504	8.0E-5	2.9790	0.0567	2000407	2.0E-5	2.9778	0.0665
0.008	2000506	1.6E-4	2.5015	0.0594	2000409	4.0E-5	2.5000	0.0756
0.010	2000508	2.0E-4	2.3492	0.0551	2000411	5.0E-5	2.3476	0.0740
0.020	2000510	4.0E-4	1.9149	0.0303	2000413	1.0E-4	1.9130	0.0611
0.040	2000513	8.0E-4	1.5593	-0.0004	2000415	2.0E-4	1.5584	0.0494
0.080	2000515	1.6E-3	1.2882	-0.0348	2000417	4.0E-4	1.2909	0.0466
0.120	2000517	2.4E-3	1.1729	-0.0558	2000419	6.0E-4	1.1798	0.0541
0.160	2000519	3.2E-3	1.1147	-0.0772	2000421	8.0E-4	1.1259	0.0663
0.200	2000521	4.0E-3	1.0869	-0.0836	2000423	1.0E-3	1.1017	0.0816

T-joint with angled crack in corner of weld, mesh 4b, load-case bending

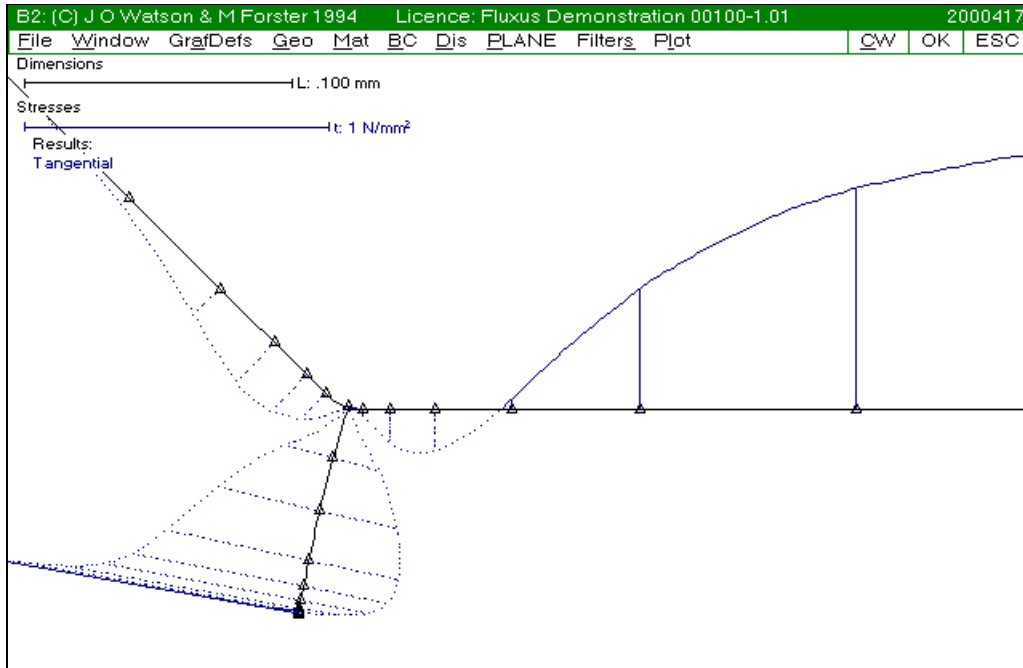
There is little difference between the straight and curved cracks. For small a/T the straight crack leads to smaller mode-II values and for large a/T the curved crack leads to smaller mode-II values. The mode-II values are no more than 2% of the mode-I values for most crack lengths, except for the longer cracks under bending and straight medium to long cracks under tension.

According to the principal stress criterion, cracks grow in such a way that the mode-II value becomes zero.

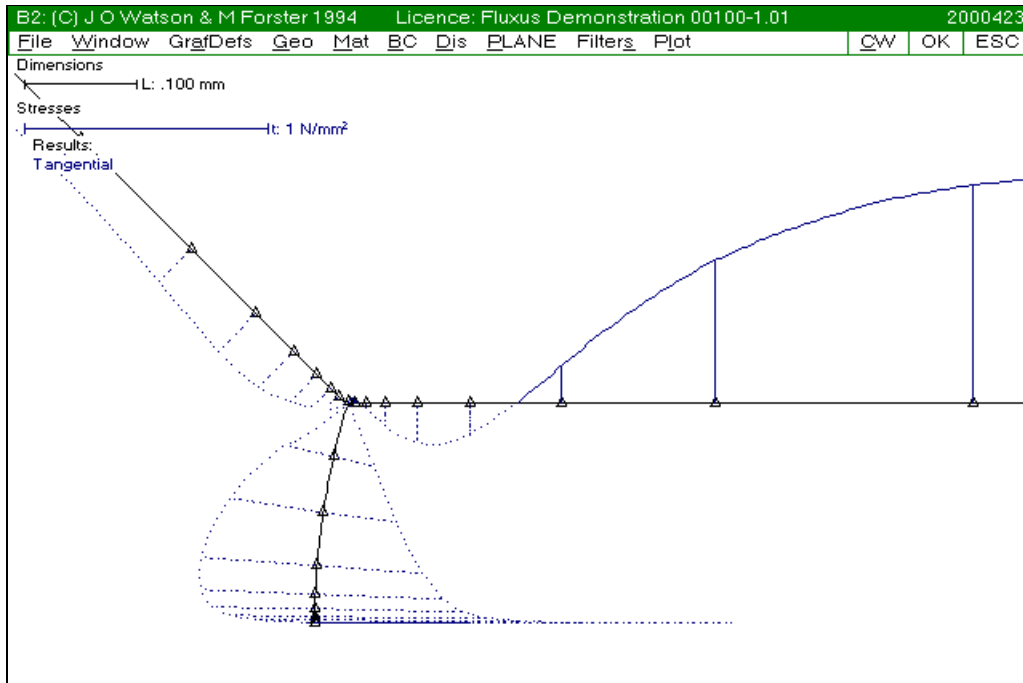
Compared to a vertical straight crack, there is much difference for short crack lengths and little difference for long crack lengths. For example, the mode I stress intensity factor for vertical cracks is 30% higher for $a/T = 0.001$, and about the same for $a/T = 0.200$. For the vertical crack, the mode II stress intensity factor is between 10% and 20% of the mode I stress intensity factor for nearly all cases except for the very long cracks under load-case tension.



Crack length 0.001 mm. Note perfect symmetry of crack stress distribution.



Crack length 0.080mm. Curved crack. Crack stress distribution symmetric along most of crack length.



Crack length 0.200mm. Curved crack. Crack stress distribution symmetric along most of crack length.